CHAPTER 8
DISCUSSION

8.1 Role of orthogneisses in the context of UHT metamorphism of the EGP

Orthogneissic rocks, particularly charnockite and granite, are common members of regional granulite terranes, and the Eastern Ghats Province (EGP) is no exception to that. These rocks form an essential component of the litho-assemblage and play pivotal role in development of the orogenic crust (Duchesne and Wilmart, 1997). The massif-type charnockite, reported in this study, covers a vast area of the EGP, though the outcrop density is not uniform throughout the terrane. This rock is closely linked with granitoids and metasedimentary rocks like khondalite and calc-silicate granulite. Based on field features, textures and geochemical characters, this charnockite has been identified as a magmatic rock that has intruded the UHT metamorphosed sedimentary rocks of the EGP. This is also vindicated by the occurrences of metasedimentary enclaves within the charnockite similar to that reported by Ganguly et al. (2017). Moreover, this charnockite magma also contained xenoliths/enclaves of mafic granulites of various sizes and shapes. Based on structural history of the EGP, the intrusion of charnockite magma occurred after the D_2/D_3 deformation events (Ganguly et al., 2018, 2021). This rock has the characteristic mineral assemblages of granulite facies metamorphism and exhibits variation in composition due to magmatic differentiation, with or without the influence of crustal contamination (Rajesh, 2012). The present investigation suggests that the massif-type of charnockite has suffered certain degree of metamorphic recrystallization as evident from the granoblastic texture. Although the rock is mostly massive in character, a crude foliation has also developed in a few places. These features are frequently associated with elongated porphyroblasts and feldspar augen, especially in proximity to ductile shear zones. Although this rock has undergone granulite facies metamorphism, they retain traces of their original igneous textures. Textural clues, such as the development of garnet corona (Grt_2) surrounding ilmenite and orthopyroxene, as well as the transformation of porphyroblastic garnet (Grt_1) into biotite + quartz symplectite, suggest a subsequent retrogressive cooling in presence of an aqueous fluid either by melt-back reaction or by later infiltration. Using suitable geothermobarometer, the maximum temperature and pressure of metamorphism is 910°C and 9 kbar, respectively. Some samples exhibit textures that include the transformation of biotite into a symplectic intergrowth of Ilm + Kfs, indicating a process of initial reheating of the cooled charnockitic lower crust. This texture suggests that the once-cooled charnockite magma underwent

a reworking, potentially associated with the M_2 metamorphic cycle at ca. 950–900 Ma, as suggested by Bose et al. (2022). This process primarily involves a dehydration melting occurring simultaneously with the movement of trace elements leading to development of zircon overgrowths and patches, as described in chapter 7. It is worth noting that this particular texture is sporadic, suggesting that the charnockite magma was devoid of water, and cooling took place within an overall H_2O-deficient environment although development of biotite indeed involved some amount of H_2O during cooling. The origin of the parent rock responsible for generating charnockite magma has been a subject of debate, as discussed by Frost and Frost (2008). However, theoretical modeling adopted in this study that focuses on partial melting of hydrated basaltic rock in a carbonic fluid regime (Fig. 5.29) could be considered as a viable model for the formation of charnockite magma within a subduction environment.

Zircon U-Pb data obtained from representative charnockite samples reveal two separate crystallization ages of the magma. While two samples yield crystallization ages in the frame of ca. 1020–1000 Ma, the remaining six samples indicate crystallization ages in the range of ca. 980–940 Ma. It is noteworthy that the age of the first pulse of charnockite magmatism closely matches with the UHT metamorphism of the EGP (Bose et al., 2011, 2022; Das et al., 2011; Korhonen et al., 2013). In contrast, the second and final pulse of charnockite magmatism occurred in the inter-kinematic gap of M_1 and M_2 metamorphic cycles (Bose et al., 2022). This implies a temporal gap of approximately 40 Ma between two separate episodes of charnockite magmatism in the EGP. The second pulse of charnockite magmatism thus occurred when the lower crust was still hot and undergoing thermal relaxation following the UHT metamorphism. Previous geochronological data also indicated the occurrence of charnockite magmatism in the EGP at ca. 980–960 Ma (Paul et al., 1990; Ganguly et al., 2018; Rajesh, 2012). The current dataset further corroborates the regional occurrence of charnockite magma in the EGP in the ca. 980–940 Ma timeframe. Zircon analyses from the overgrowth and patchy domains yield nearly concordant spot dates ranging from ca. 950 Ma to ca. 750 Ma. These dates could be associated with subsequent metamorphic events, such as the M_2 metamorphism at ca. 950–900 Ma (Bose et al., 2022), and/or partial modification of older zircon by fluid-related processes at ca. 550–500 Ma (Das et al., 2021). It is worthwhile to mention that the associated granitic rocks show crystallization age of ca. 987 Ma (Bose et al., 2011) which is broadly coeval with the age of charnockite magmatism and the former rock also exhibits various evidences of metamorphism.

Since the emplacement temperature of charnockite magma reaches ~1000°C (Kilpatrick and Ellis, 1987), such magma has a potential to cause HT to UHT metamorphism. In some cases, charnockite magmas are considered as heat sources UHT metamorphism (Schorn et al., 2020). On the other hand, charnockite magma has been considered as a product of UHT metamorphism in many terranes (Rajesh et al., 2014; Klaver et al., 2015). Since the majority of the charnockite and granite of the EGP were emplaced after the UHT metamorphism, it is implied that the magmatic rocks have not served as heat sources for the UHT metamorphism. Notably, the most prominent age clusters for orthogneisses are identified to have formed approximately 20-40 Ma after the UHT metamorphism event, indicating that they are more likely a consequence rather than cause.

8.2 Geochemical evolution of the felsic gneisses and its tectonic implication

In order to understand paleotectonic setting for felsic magmatism, geochemical tools play a vital role. Interestingly, the charnockite-granite association of the EGP shows comparable geochemical similarities which can be evident from Tables 5.4 and 5.5. These two rocks show broad range of SiO_2 (charnockite: 53-72 wt.% and granite: 57-76 wt.%), but variation in terms of K_2O (charnockite: 1.36-5.14 wt.% and granite: 3.46-7.66 wt.%) and FeO_T (charnockite:2.76-9.66 wt.% and granite: 0.99-7.96 wt.%). Charnockite samples exhibit distinctive features such as elevated levels of K_2O, P_2O_5, and TiO_2, along with reduced CaO and Mg# when compared to the I-, S-, and M-type variants, all at a consistent SiO_2 content. The elevated levels of P_2O_5 and TiO_2 are evident through the significant modal percentages of Fe-Ti oxides and apatite, respectively. In terms of composition, both the high-SiO_2 and low-SiO_2 charnockite samples are compositionally granitic to granodioritic, in contrast to the quartz monzonitic type reported by Rajesh (2012). Both varieties exhibit a mix of ferroan and magnesian characteristics, making them transitional or intermediate types, as observed in earlier studies (Rajesh, 2012; Frost and Frost, 2008). Interestingly, the representative granites show somewhat similar character. Charnockite samples show metaluminous to weakly peraluminous character while the granite samples are mainly peraluminous and both the rock types show calcic, alkali-calcic, to alkalic nature. The inverse relationships observed in charnockite between CaO, FeO_T, MgO, TiO_2, and P_2O_5 and SiO_2 go with early pyroxene, Fe-Ti oxide, and apatite fractionation during magma evolution. Conversely, the negative correlation between SiO_2 and Al_2O_3 suggests a limited degree of feldspar fractionation, a finding substantiated by the weak correlations among K_2O, Na_2O, and Al_2O_3, as well as the

moderate presence of Eu anomalies (average Eu/Eu* = 0.66). The absence of negative correlations among CaO and Al_2O_3, CaO and Na_2O, Na_2O and Al_2O_3, as well as Eu/Eu* and Sr, and the absence of correlation between CaO and Sr, indicate that plagioclase fractionation did not occur extensively. Nevertheless, the presence of Eu anomalies does raise the possibility of plagioclase fractionation unless these anomalies would originate from a partial melt source. The granite samples also show weak negative Eu anomalies possibly for the same reasons. The REE plots of the charnockite-granite association show similar LREE-enrichment and HREE-depletion trends. However, discrepancies exist as a few charnockite samples show somewhat flat trend while one granite show HREE enriched trend. The charnockite samples are notable for their significant concentrations of Ba and they exhibit enrichments in Pb, La, Nd, and Gd, while displaying depletion of Nb, Ta, Sr, and Ti. In contrast, the granites show enrichment of Rb, Th, K, Pb, Li and depletion of Ba, Nb, Ta, Sr, P and Ti. Additionally, there are subtle depletion of Ce and Y. All these evidences (Yang et al., 2016; Hollocher et al., 2012) collectively suggest of an arc setting for generation of the charnockite-granite magma of the EGP. The abundance of Rb and K is likely associated with a rise in the proportion of alkali elements. The significant divergence in magma composition may have led to enrichments in Zr and Hf. It is noteworthy that most samples from both the rocks exhibit a negative Sr anomaly, which could be inherited from the extensively fractionated mantle source (Tang et al., 2015).

Trace element and REE characters of zircon in the charnockite samples also provide distinct clues to the tectonic setting for magmatism. The distinct patterns are observed in the trace and REE data obtained from both magmatic and overgrowth/patchy zircon domains from charnockite. The presence of negative Eu and Ti anomalies in the LREE-depleted and HREE-enriched magmatic zircons suggests that magma formation occurred at a lower crustal depth, where the fractionation of plagioclase and Fe-Ti oxides took place (Belousova et al., 2002). Conversely, the elimination of the Ce anomaly, the more subdued LREE, and the upwardly curving HREE patterns suggest the re-mobilization of these elements during metamorphic recrystallization (Hoskin and Black, 2002).

Comparing published petrological and high-resolution geochronological results from the EGP (Mezger and Cosca, 1999; Upadhyay et al., 2009; Bose et al., 2011; Das et al., 2011; Korhonen et al., 2013; Ganguly et al., 2018), it can be inferred that EGP underwent a geological evolution involving subduction, accretion, and collision within the timeframe of ca. 1030–900 Ma

which matches with the already established models (Dasgupta et al., 2013, 2017; Bose and Dasgupta, 2018; Ganguly et al., 2021; Bose et al. 2022).

Furthermore, geochronological data also indicate an event of rifting of the EGP during the time frame ca. 1400–1250 Ma, characterized by the intrusion of mafic and alkaline magmas (Upadhyay, 2006; Ranjan et al., 2018). Recent findings also reveal the presence of felsic magmatism during ca. 1230–1180 Ma in the northern part of the EGP, suggesting the formation of an ensialic basement over the previously rifted basin (Ganguly et al., 2018; Bose et al., 2021; Banerjee et al., 2023).

8.3 Charnockite magmatism in EGP and Rayner Province

It is already established that the EGP and Rayner Province of East Antarctica has a shared geological history during the time frame ca. 1000-900 Ma (Harley, 2003, Harley et al.,2013; Dasgupta and Sengupta, 2003; Mezger and Cosca, 1999; Bose et al., 2011; Dasgupta et al., 2013, 2017; Morissey et al., 2015; Bose and Dasgupta, 2018; Bose et al., 2022). Geochronological data of the present study show two distinct age groups for charnockite magmatism in the EGP. While the first phase of charnockite magmatism (ca. 1020–1000 Ma) is broadly synchronous with the UHT metamorphism (Bose et al. 2011, 2022; Das et al., 2011; Korhonen et al., 2013), a more extensive phase of magmatism (ca. 980-940 Ma) occurred in the interkinematic gap between the M_1 UHT metamorphism (ca. 1030-990 Ma) and the M_2 metamorphism (ca. 950–900 Ma) as reported in recent studies (Bose et al., 2022). This implies a protracted thermal history of the EGP punctuated by charnockite magmatism. Similar episodic charnockite magmatism has also been reported from the Mawson coast of Rayner Province of East Antarctica. Areas like McRobertson Land, Kemp Land and Enderby Land witnessed charnockite magmatism (Mawson charnockite) at ca. 1145-1140 Ma, ca. 1080-1050 Ma and ca. 985-960 Ma (Halpin et al., 2012). These charnockites occupy significant geographical areas of the Rayner Province covering more than 3,000 km^2 (Young and Ellis 1991; Sheraton and Black, 1988; Halpin et al., 2012). Given its spatial distribution, albeit in isolated occurrences, it is conceivable that the extent of charnockite magmatism in the Rayner Province may exceed 5,000 km^2, as previously anticipated (Young and Black, 1991). The reported ages of Halpin et al. (2012) coincides with the ages of charnockitic plutons in the Bunger Hills region of the Wilkes province (ca.1170-1150 Ma; Sheraton et al., 1992). Notably, charnockites found in MacRobertson Land and Bunger Hills exhibit ductile deformation

along their periphery and are regarded as being syn- to late-tectonic (Young and Ellis, 1991; Kilpatrick and Ellis, 1992; Sheraton et al., 1992). Intrusions of syn- to late- kinematic granites and charnockites are also reported from northern Prince Charles Mountain (nPCM) approximately at ca. 1050-950 Ma age (Kinny et al., 1997). Considering the regional extent (Fig. 8.1) incorporating the EGP and the Rayner Province as a composite arc terrane, this magmatism would span a geographical width exceeding 500 kilometers (Liu et al., 2014). This huge continental arc system is separated by an oceanic or back-arc basin from the Indian craton (Liu et al., 2017). Furthermore, the recorded ages of orthogneissic rocks in various sectors, encompassing both the central and northern parts of the EGP and the Rayner Province, suggest their emplacement in an episodic fashion within an arc system.

The charnockite, along with its corresponding magmas, were intruded into the Rayner Province either during or right after the intense granulite metamorphism and the related D_2 deformation events (Halpin et al., 2012). These charnockite bodies are intrusive, foliated, medium to coarse grained gneiss with or without megacrysts of K-feldspar (<6-7cm in length) that are aligned parallel to retrograde biotite foliation, equivalent to regional S_3 (White and Clarke, 1993). Subsequently, these rock formations experienced deformation from two subsequent events, namely D_3 and D_4 (Halpin et al., 2012). This magma also includes patches and inclusions of pelitic and calc-silicate granulites, as reported by White and Clarke (1993). According to their observation on Mawson charnockite found in the Colbeck archipelago, this rock constitutes a substantial intrusive mass along the Mawson Coast. The charnockite magma, which was notably dry, intruded the supracrustal sequence at temperatures exceeding 1000 °C (Young and Ellis, 1991). This intrusion process essentially led to the dehydration of the crust. The peak metamorphic temperature conditions have been estimated close to 850°C and pressure close to 5.6-6.2 kbar (Halpin et al., 2007) which is lower than the temperature and pressure estimated from EGP indicating much shallower depth of metamorphism for Mawson charnockite. The geochemical analysis of the Mawson charnockite in the vicinity of nPCM reveals trace element features, such as relatively moderate negative Sr anomalies, which align closely with the characteristics of Si-rich granulites. This suggests that these rocks likely share a common origin in a tectonic scenario reminiscent of a subduction-type setting, resembling modern arc environments (Munksgaard et al., 1992). On the other hand, charnockites in the McRobertson Land region exhibit low levels of alkali components and are primarily composed of magnesian minerals. They display characteristics ranging from

metaluminous to weakly peraluminous, with features that include calc-alkalic, alkali-calcic, and calcic properties. In tectonic context, these charnockite is believed to be late in the orogenic process, with the magma intruding during a period of compression within an accretionary environment (Mikhalsky et al., 2006). The magmatic charnockites in the Mawson Coast region exhibit geochemical differences related to their TiO_2 content, distinguishing between high-Ti and low-Ti varieties. However, it is noteworthy that both of these variations share similar Sr-Nd isotopic characteristics (Young et al., 1997). According to Zhao et al. (1997), the magmatic charnockites in the nPCM region exhibit geochemical resemblances to those found along the Mawson Coast. Nevertheless, they display isotopic differences, featuring consistent initial $^{87}Sr/^{86}Sr$ ratios ranging from 0.7063- 0.7100, initial εNd values spanning from -4.0 to -5.9, and Nd-depleted mantle model ages between 1.60-1.98 Ga. These characteristics suggest that these charnockites are likely to have originated from pre-existing crustal sources associated with subduction-collision events. Overall, Mawson charnockites tend to exhibit lower Rb/Sr ratios but higher K/Rb and Sr/Ba ratios. They also have higher concentrations of Ba, Rb, and Sr, while showing lower levels of U, Th, Nb, La, and Y in spider plots, in comparison to the EGP charnockites. These observations suggest that charnockites from Mawson may have undergone relatively less differentiation.

In the Prydz Bay and Amery Ice Shelf regions of East Antarctica, situated along the eastern margin of the Rayner Province, the Rayner orogenic cycle unfolded through three distinct tectonic phases (Mikhalsky et al., 2018). These phases are identified as follows: the Fisher phase, spanning approximately from 1200-1100 Ma; the Beaver phase, occurring within the timeframe of 1000-950 Ma; and the Bolingen phase, taking place from 900-800 Ma. Some researchers propose a two-stage evolution of the Rayner Province in this region. This perspective posits an initial arc-continent collision around 1000-970 Ma, succeeded by a subsequent continent–continent collision approximately between 940-900 Ma (Kelly et al., 2002; Halpin et al., 2007; Liu et al., 2013, 2014). The dual-cycle narrative bears a striking resemblance to the one presented for the EGP earlier. Nevertheless, in this specific segment of the Rayner Province, there is a notable absence of definitive and conclusive proof of a collisional suture, with the exception being the presence of ultramafic slabs in the Lawrence Hills and Radok Lake areas (Mikhalsky et al., 2018). These intersecting arcs, specifically the Fisher arc (ca. 1380–1200 Ma), the Clemens arc (ca. 1080–1030 Ma), and the Rayner arc (ca. 1000–970 Ma), underwent successive development (as illustrated in

Fig. 8.2). This development was accompanied by processes such as back-arc sedimentation, magmatic activity, and metamorphism (Mikhalsky et al., 2006, 2018; Liu et al., 2014). Considering the similarities in their tectonic backgrounds, Liu et al. (2014) contended that the Rayner Province and the EGP comprised a substantial, contiguous continental arc, spanning approximately 500 kilometers in width. Furthermore, the detrital zircon age signatures obtained from various regions including the Larsemann Hills, Bolingen Islands (Kelsey et al., 2008; Wang et al., 2008; Grew et al., 2012), the Eastern Amery Ice Shelf (Liu et al., 2009, 2014), the Kemp Land and Napier Complex (Kelly et al., 2002; Halpin et al., 2005), exhibit notable similarities with those found within the EGP, as highlighted in earlier studies (Bose et al., 2011; Das et al., 2011). Additionally, the Pb isotopic compositions of K-feldspar, as studied by Flowerdew et al. (2013), also align with these similarities. Considering the notable absence of these age signatures in the even older Lambert and Ruker provinces, it was suggested that the sedimentary material in the Rayner-Eastern Ghats terrane (R-EG) primarily originated from the Indian cratonic margin (Corvino et al., 2011; Grew et al., 2012; Liu et al., 2014; and Bose and Dasgupta 2018). This hypothesis finds further support in the presence of ca. 1400–1200 Ma old mafic dikes observed in the Napier Complex (Suzuki et al., 2008), the Vestfold Block (Black et al., 1991), and the related mafic and alkaline magmatism in the EGP (Ranjan et al., 2018). Thus, the development of the Rayner Province can be attributed to the eventual collision between the Indian continent (comprising the Dharwar, Bastar, and Singhbhum cratons) and the East Antarctic continent (encompassing the Lambert and Ruker provinces). This collision occurred either through an extended geological process, as suggested by Boger et al. (2000) and Carson et al. (2000), or in two distinct phases, as more recently proposed by Bose et al. (2022). The latter two-cycle model receives additional support from the differing patterns of pressure-temperature (P-T) paths observed in the Rayner Province. Specifically, a clockwise P-T path has been documented in the Kemp Land region, while an anticlockwise P-T path has been observed in the McRobertson Land areas (Kelly et al., 2002; Halpin et al., 2007; Liu et al., 2013, 2014). This is similarly applicable to the EGP also, where the M_2 metamorphism exhibits a clockwise P-T path that overlays an earlier anticlockwise P-T path associated with the M_1 metamorphism (Das et al., 2011; Bose et al., 2022). It is likely that the M_2 cycle played a role in bringing the deep crustal charnockites and other lower crustal rocks to their current exposed surface.

The concluding episode in the India-East Antarctica sector marked the ultimate collision that had a profound impact on the entirety of the R-EG, resulting in extensive metamorphism, deformation, and magmatic activity (Fig. 8.1). In this tectonic context, the Mawson-EGP charnockites, along with granitoid magmas, underwent intrusion into the lower crust of the R-EG during at least three distinct phases (Fig. 8.2). The first phase of charnockite intrusion (ca. 1145–1140 Ma) occurred as a late orogenic magma within the Fisher arc. Notably, there are no recorded instances of charnockite within the EGP from this phase, suggesting that the Fisher arc was situated quite a distance away from the EGP during this period. However, slightly older charnockite magmatism (ca. 1200-1220 Ma) has been recently discovered in the Angul domain (Bose et al., 2021; Banerjee et al., 2023). The second phase of charnockite intrusion (ca. 1080–1050 Ma) took place within the Clemens arc. The ultimate phase, known as phase-3, saw the intrusion of charnockite across a wide expanse of the Rayner-EGP arc, occurring roughly between 985-940 Ma. The charnockite and the accompanying granitoid magmas, as exemplified by the 987 Ma granite described by Bose et al. (2011), were emplaced during a compressional orogenic event, during which the lower continental crust underwent significant shortening (Ganguly et al., 2021). The ultimate collision event between the Rayner-Eastern Ghats Province (R-EG) and the Indian craton marked the conclusive closure of the oceanic basin that once separated them. The currently exposed R-EG region can be seen as a transformation from formerly active arc systems (comprising the Rayner-EGP arc, Clemens arc, and Fisher arc), now characterized by the presence of charnockite-granite arc magmas. This study, in particular, uncovers a significant causative relationship between the two distinct cycles of metamorphism and the interceding charnockite magmatic activity. These geological processes unfolded within a subduction-accretion-collision context that intimately involved the Indian continent and the R-EG arc system.

8.4 Diversity of felsic magma: granite vs. charnockite

Granitic rocks are closely linked with charnockite in regional granulite terranes. These two rocks are commonly regarded as distinct outcomes arising from the differentiation of single felsic magma having contrasting fluid environments (Harlov et al., 2013). In the context of EGP, a similar argument can be put forward. Both rock suites exhibit substantial volume but they do not exhibit any direct contact or intrusive mutual relationship, nor do they contain any enclaves or xenoliths of one another. Many researchers (Frost et al., 2000; Elliott, 2003; Frost and Frost, 2008; Harlov

et al., 2013) have proposed that the correlation between charnockite and granite can be elucidated by considering the dual nature of the fluid regime. Typically, the fluids commonly observed alongside a granitoid melt primarily comprise H_2O, CO_2, and saline fluids containing NaCl, KCl, and $CaCl_2$ (Brown 2013; Manning 2018). Where H_2O is the most dominant fluid species during magmatic crystallization, the fluid-bearing Fe–Mg silicate minerals are represented by biotite or amphibole. The rock suite is then dominated by hornblende-and biotite-bearing granites. Conversely, where the a_{H2O} falls significantly below 1, orthopyroxene and, in some instances, clinopyroxene would predominate as stable Fe–Mg silicate phase throughout the course of evolution in the same continuum by the following reactions:

Bt + Qtz = Opx + Kfs + H_2O …………………………... (8.1)
Hbl + Qtz = Cpx + Opx + Pl + Kfs + H_2O………………... (8.2)
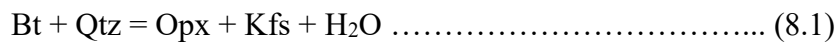
The rock suite is then dominated by charnockite containing Opx with or without Cpx. A reduced a_{H2O} typically signifies an elevation in the proportions of CO_2 and/or saline components like NaCl, KCl, and $CaCl_2$ in the fluid accompanying the melt (cf. Frost et al. 2000; Frost and Frost 2008; Manning 2018). The magma residing deep below would gradually dissolve a greater amount of CO_2, which would then be liberated at shallower depths through exsolution during its ascent (Frost et al., 2000). The size of the respective regions occupied by charnockite and granite would depend on the P-T-X conditions, as well as the initial H_2O/CO_2 ratio of the melt during both magmatic crystallization and subsequent cooling and uplift. The H_2O/CO_2 ratio in a granitoid melt is heterogeneous. If the ratio is primarily influenced by H_2O within the melt, the likely outcome is the crystallization of only granite or granitoid rocks. When CO_2 dominates, magmatic charnockite formation is more probable. In cases where both H_2O and CO_2 are present in broadly equal proportions, the result will likely be the crystallization of granite or granitoid rocks alongside areas where charnockite forms (Harlov et al., 2023). Numerous natural analogs have been used to test the validity of this hypothesis. Recent work of Harlov et al. (2023) on Weinsberg granite and associated charnockite supports this hypothesis. These workers have found highest number of carbonic fluid inclusion within charnockite along with NaCl brine whereas granitic counterpart is dominated by H_2O fluid inclusion with $CaCl_2$ brine component. Similar cases have been reported from other areas like VerburgTorpa (Harlov et al., 2013), Bohemian Massif (Finger and Clemens, 1995; Klötzli et al., 2001; Finger et al., 2003), Rogaland Igneous Province (Madsen, 1977;

Petersen, 1980), Louis Lake Batholith (Frost et al., 2000), Planalto granite suite and Amazonian craton (Feio et al., 2012).

8.5 Mafic magmatism in the EGP

Mafic granulite plays an important role in the evolution of regional granulite terranes serving as a witness to the interplay between the lower crust and the sub-lithospheric mantle (Harley 1989). This rock normally occurs in two forms: either as a mafic magmatic rock that has subsequently experienced intense metamorphism and complete recrystallization (Harley 1989; Montanini and Tribuzio 2001; Faryad and Hoinkes 2004) or as a basic sedimentary rock that undergoes dehydration melting (Beard and Lofgren 1991; Pattison 1991; PatiñoDouce and Beard 1995; Springer and Seck 1997). In the latter case, the rock is usually found as enclaves in felsic granulites without showing intrusive relation. The present study focuses on investigating both the forms of mafic granulites. The first category comprises the massive two pyroxene-bearing mafic granulite reported from various localities of the EGP (Shaw et al., 1996; Dasgupta et al., 1991, 1993; Bose et al., 2003). It has been established that this rock originated from a mafic magmatic protolith that intruded the deep continental crust before undergoing UHT metamorphism (Dasgupta et al. 1993; Bose et al., 2003; Bose et al., 2011b). A comparable evolutionary history is suggested for the present massive variety of mafic granulite studied here. Shaw et al. (1997) presented geochronological evidence that mafic magma intruded the lower crust around 1450 Ma in the Rayagada region of the EGP. Similarly, the Anakapalle locality of the EGP reported emplacement of mafic magma around ca. 1580 Ma (Kelsey et al. 2017). Recent tectonic modeling suggests that the metamorphism of the EGP took place in an accretionary tectonic setting, coinciding with rifting and the opening of the back arc basin (Dasgupta et al. 2013, 2017; Bose and Dasgupta, 2018). The sediments that were deposited within the back arc basin along with the mafic and alkaline magma (emplaced at ca. 1.48–1.30 Ga, Upadhyay 2008; Ranjan et al. 2018) and suffered UHT metamorphism along an anticlockwise path during 1030–990 Ma (Bose et al. 2011; Das et al. 2011; Korhonen et al., 2013b). This anticlockwise path possibly indicates significant magmatic activity during or after tectonic crustal thinning (magmatic intra- or under-plating), which is typical of a magmatic arc (Abati et al. 2003). Therefore, it is possible that some of the massive variety of mafic granulite has a magmatic source which was emplaced around ~1000 Ma. However, no age data has been reported so far to make a conclusion on this issue.

On the other hand, the garnet-bearing mafic granulite (migmatitic variety) is less abundant in the EGP, and its evolutionary history is not well-documented. It is likely to have formed from anatexis of a mafic protolith, a process documented in other metamorphic terranes (Brown 1994; Dziggel et al. 2012; Feisel et al. 2018). Experimental data shows that mafic protolith melts at temperatures above 800°C, with more than 10% of the melt produced at temperatures over 850°C, under pressures ranging from 5-10 kbar (Beard and Lofgren 1991; Rushmer 1991; PatiñoDouce and Beard 1995; López and Castro 2001). In all the experiments, the resulting melt exhibits a tonalitic–trondhjemite composition, while the solid residue comprises a combination of orthopyroxene, clinopyroxene, and plagioclase, sometimes with garnet. A significant textural indicator of anatectic mafic migmatite is the persistence of residual hornblende within garnet (Hartel and Pattison 1996). The lack of hornblende within porphyroblastic garnet in the present case makes it impossible to furnish direct textural confirmation of anatectic origin of mafic granulite. One potential explanation is that the peritectic melting reaction, which consumes hornblende, progressed into the realm of UHT metamorphism without leaving any remnants behind. Conversely, textual indications such as the presence of a thin K-feldspar film on plagioclase and the presence of quartz provide support for the initiation of melting. Conventional thermobarometric data suggests the peak metamorphic temperature at 8 kbar pressure is around 890°C, but this may be a reset value since mafic granulites from nearby locations indicate higher temperature estimates (Dasgupta et al. 1991, 1993; Bose, 2003). Additionally, presence of orthopyroxene lamellae within clinopyroxene in the studied samples provides fossil evidence of UHT metamorphism (Frost and Chacko, 1989; Harley, 2008).

8.6 Fluid evolutionary history of the lower crust

Oxide-sulphide-silicate mineral associations from mafic granulites have been used to understand the fluid-rock interaction in the lower crustal condition. Two types of mafic granulite reported in this study containing stable mineral assemblage like clinopyroxene + orthopyroxene + plagioclase + ilmenite ± garnet ± magnetite ± pyrrhotite, chalcopyrite ± pyrite (Py_1) at the peak metamorphic condition. The primary mineral composition observed during the peak stage consists mainly of ilmenite (Ilm_2), either in isolation or coexisting with discrete magnetite. In cases where magnetite is found alongside ilmenite, it lacks exsolved ilmenite within it. Consequently, the separation of these two oxides through the process of unmixing from an oxide solid solution, as proposed by

Vincent and Phillips (1954) does not appear to be a viable mechanism for the formation of this dual-oxide aggregate. In contrast, the close connection between discrete magnetite (Mag_2) and Ilm_2 suggests the potential stabilization of the former in the oxidized samples through reaction (6.1). In all of the assemblages, there is an absence of distinct hematite grains, indicating that the fO_2 condition never reached the HM buffer range during the metamorphic evolution. In sample 9C, hemo-ilmenite (Ilm_2) is found alongside Mag_2 in the matrix within a comparatively more oxidized assemblage. This suggests variations in the fO_2 conditions among different samples, with fluid composition predominantly influenced and stabilized by mineral assemblages. In a complex, multicomponent fluid system, such fluctuations in fO_2 are likely to be influenced by the fugacities of other components. According to the composition of pyrrhotite and the calculated sulfide phase relationships (Toulmin and Barton 1964), the estimated fS_2 values vary within the range of -3.50 to -3.67 under the relevant temperature conditions (Table 6.6).

Sulfide phases are predominantly composed of either pyrite (in samples 17EG16 and 9C) or pyrrhotite (in samples 17EG14, 17EG22, 17EG23, and 17EG24). When examining a temperature versus fO_2 plot using QUILF equilibria (Andersen et al. 1993), it becomes evident that pyrrhotite-bearing assemblages exhibit lower fO_2 values compared to those containing pyrite. According to experimental data, temperature above 743°C, the stability of sulfide phases in mafic rocks is contingent upon the prevailing fO_2 conditions. Beyond this temperature threshold, pyrrhotite becomes the stable phase in favor of pyrite, regardless of the specific fO_2 values (Kullerud, 1957). Hence, it can be inferred that pyrrhotite is expected to be the stable phase during the peak of UHT metamorphism in both assemblages. In contrast, both Py_1 and Py_2 phases must have formed at temperatures lower than the metamorphic peak. The fO_2 values calculated for samples characterized by pyrite-dominated assemblages are consistently 3 to 4 log units higher than the FMQ buffer. Another noteworthy aspect is the emergence of Py_2 and Mag_3 during the retrograde phase of metamorphism, a development likely influenced by cooling under conditions of elevated fO_2.

Maintaining an elevated oxygen fugacity in the lower crust can be accomplished through various means:

1. High fO_2 mineral assemblages in the lower crust can be inherited from an oxidized protolith, as demonstrated by Arima et al. (1986) in the case of metapelitic granulite. With

the basic magma as the protolith for the massive variety of mafic granulite taken into consideration, the potential for inheriting highly oxidized mineral assemblages is being investigated. In the lower crustal condition processes like partial melting and melt segregations are the important factors that regulate the fO_2 condition in basic magma (Ballhaus 1993; Zhang et al. 2013). The phase relationships within the FeO-Fe_2O_3 system indicate that magnetite can remain a stable mineral alongside hematite at temperatures reaching approximately 1530°C as the fO_2 levels increase (Darken and Gurry 1945; Muan 1958). Experimental evidence indicates that basic magma within arc settings exhibits a higher level of oxidation when compared to magma in other tectonic environments (Carmichael, 1991; Ballhaus, 1993). The geochemical characterization of mafic magmatism in the EGP lacks robust constraints, and the existing data point to a potential extensional setting likely occurring around 1580–1350 Ma (Shaw et al., 1997; Kelsey et al., 2017; Ranjan et al., 2018). Conversely, the extended subduction-accretion history of the EGP is indicated by metamorphic and geochronological records, spanning approximately ca. 1200 to 900 Ma (Dasgupta et al., 2013, 2017; Bose and Dasgupta 2018). During this period, there was a notable occurrence of high-temperature metamorphism, significant deformation, and the emplacement of granitoids displaying characteristics typical of volcanic arcs (Saha and Karmakar, 2015). It is plausible that the chemical composition of mafic granulites in EGP might have been altered by arc magmas. Some of the rhombohedral oxides could potentially have been inherited from a magmatic source. Unfortunately, due to the lack of precise geochemical data, this hypothesis cannot be further investigated.

2. Another potential explanation for the elevated fO_2 in lower crustal rocks is the influence of internal fluid buffering. The high oxidation states observed in the minerals of samples 17EG16 and 9C may be attributed to an oxidized protolith with internal mechanisms for oxygen buffering during metamorphism. This process appears to be the predominant one in the case of the present samples. Conversely, features such as Mag_4 veins, Py_2 rims on Po, and alteration textures are more likely to have formed at a later stage due to the influence of an external fluid source.

3. The third potential explanation involves an external fluid source. The process of oxidation by an infiltrating fluid during granulite facies metamorphism has been a subject of limited

clarity for an extended period. While CO_2 and H_2O are not particularly effective as oxidizing agents in rocks devoid of graphite (Frost, 2018), the presence of the SO_2 component in brine may play a significant role as an oxidizing agent (Crawford and Hollister, 1986; Stout et al., 1986; Cameron and Hattori, 1994; Harlov et al., 1997; Newton and Manning, 2005; Harlov, 2012). In a subduction-accretion environment, fluids originate from the dehydration of the intensely heated subduction zone and primarily consist of H_2O, along with dissolved solutes such as Ca and Al (Manning, 2004; Zheng et al., 2016). This hydrothermal supercritical fluid serves as an optimal medium for material transportation, including sulfates, due to the presence of alkali chloride components within it (Keppler, 1996; Ni et al., 2017; Barnes et al., 2018). In a halogen-rich aqueous fluid of this nature, the formation of ion pairs ($NaCl_{aq}-KCl_{aq}$) is facilitated at elevated temperatures, and calcium (Ca) exhibits significant mobility (Barnes et al., 2018). Additional sources of concentrated brine may include deeply buried evaporates (Yardley and Graham, 2002) or downward circulation of dissolved salts derived from surficial sources within thermally-driven convection cells (McLelland et al., 2002). However, it is worth noting that finding concrete proof of brine-rich fluid inclusions within lower crustal rocks is infrequent (Touret and Huizenga, 2012; Touret and Nijland, 2013). This scarcity might be attributed to their wetting behavior with mineral phases (Touret, 1985, Watson and Brenan, 1987; Manning and Aranovich, 2014).

The fluid inclusion data collected from various locations from EGP, viz. Chilka Lake (Bose et al., 2016), Simliguda (Bose et al., 2009), G. Madugula (Mohan et al., 2003), Paderu (Das et al., 2021) and Vizianagaram (Sarkar et al., 2003), consistently reveal the presence of CO_2-H_2O fluid compositions, but no direct evidence points to the existence of brine. Remarkably, the significant fluorine (F) content exceeding 3 wt.% in fluor-biotite (Bose et al., 2005 and Ganguly et al., 2017), as well as the substantial F content exceeding 6 wt.% in fluor-wagnerite (Das et al., 2017), within mineral assemblages, strongly suggests the potential presence of halogen-rich fluid components during both the peak and retrograde stages of metamorphism. Studies by various workers (Möller et al., 1997; Stober and Bucher 2005) suggest that mafic rocks in lower crustal condition are dominated by $CaCl_2$-rich brine solution. In the studied samples, the occurrence of patchy zoning with alternating Ca and Na concentrations in plagioclase may suggest that these plagioclase

crystals formed through interaction with a fluid enriched in brine components (Harlov, 2012). Furthermore, the widespread occurrence of magnetite veins cutting through oxide-sulfide grains and the formation of myrmekite along the interface between perthitic K-feldspar and plagioclase are likely outcomes of metasomatism induced by a fluid rich in brine components (Harlov et al., 2006; Touret, 2009; Harlov, 2012). Harlov and Hansen (2005) conducted a comprehensive investigation in Tamil Nadu, South India, and put forward the hypothesis that the observed patterns of oxide-silicate-sulfide mineral assemblages, their compositions, and textures are outcomes of brine infiltration (comprising NaCl, KCl, and oxidizing component $CaSO_4$) during high-grade metamorphism. Consequently, the elevated oxidation state observed in the rocks during retrogression may be attributed to the infiltration of a similar fluid. In a neighboring locality, it has been established that UHT metamorphism took place under elevated fO_2 conditions (approximately 3-4 log units above the FMQ buffer; Bose et al., 2009). Subsequently, evidence from fluid inclusion data indicated the infiltration of a distinct fluid phase composed of CO_2-H_2O. The latter study further suggests that the post-peak fluid composition is characterized by higher concentration of brine compared to the pre-peak fluid.

8.7 Fluid evolution in the shallow crustal level

In the garnet bearing mafic granulite (migmatitic variety), barite is observed along brittle fractures, frequently replacing both sulfide and oxide phases. It is also commonly found in conjunction with calcite in the intergranular spaces. Experimental data concerning anhydrite stability indicate that sulfate stability is promoted only when the fO_2 level is 2 log units above the FMQ buffer (Carroll and Rutherford, 1987; Török et al., 2003). Experimental findings indicate that barite tends to precipitate at relatively shallow crustal conditions (less than 400°C and 2 kbar pressure) when subjected to a high level of oxygenation (Hanor, 1994, 2000; Yardley, 2005). Given the possibility of external hydrothermal fluids playing a role in the oxidation process, they could be responsible for promoting the subsequent precipitation of barite (Ohmoto and Skinner, 1983; Shikazono et al., 1983; Van Cranendonk and Pirajno, 2004). Introduction of such a fluid may have triggered the barite precipitation along the fragile fractures within the garnet bearing mafic granulite. In such a scenario, the combination of a hot, deep-seated crustal fluid with a cooler, near-surface hypersaline brine could have led to the leaching of sulfide minerals, resulting in the release of oxygen (Valenza et al., 2000). Additionally, the elevated oxygen fugacity in shallower environments can also be

induced by bacterial processes (Hattori and Cameron, 1986). Alternative external sources may include connate fluids or reactivated meta-evaporites in the shallower crustal zones (Hanor, 2000). Shallow crustal brines might also originate from the dissolution of halite followed by subsequent evaporation and precipitation (Rittenhouse, 1967). Nonetheless, studies of fluid inclusions within a low-temperature ore field indicate that in comparison to evaporites, bittern brines are more frequently encountered in subsurface geological layers (Yardley, 2009).

8.8 Juxtaposition of EGP against the cratonic India and the effect of hot orogeny on cold lithosphere

Along the north-western margin similar type of rocks (aluminous granulite, charnockite, mafic granulite etc.) are reported. Along the western margin of the EGP, monazite ages from aluminous granulite rocks exhibit a variation in the range of approximately 1060-900 Ma which is indicative of the timeframe during which metamorphism took place for metamorphism (Simmat and Raith, 2008). It was further corroborated in later studies involving monazite and zircon (Chatterjee et al., 2017b). The latter study also identified two younger metamorphic events at ~800–750 Ma and ~530–500 Ma. These authors proposed an age zonation that is characterized by the presence of ~950–900 Ma granulite facies metamorphism in the interior part of the EGB and the 530–500 Ma event, overprinting the granulite facies metamorphism, at the zone bordering the Bastar Craton. All the geochronological data and the presented tectonic models support the theory of thrusting of the EGP over the Bastar Craton at ~550-500 Ma (Gupta et al., 2000; Das et al., 2008; Biswal et al., 2007; Bhadra et al., 2004; Chatterjee et al., 2017a; Padmaja et al., 2021). However, in some alternative theories it was argued that amalgamation of EGP and Bastar craton took place during the Tonian age formation of Rodinia and tectonothermal reworking is only restricted to shear zones only (Terrane boundary shear zone; Upadhyay et al., 2006; Chattopadhyay et al., 2015; Ranjan et al., 2018; references therein). In a recent study, Ravikant (2019) characterized the reworking event of the contact zone from the Bolangir area where the granulites of the EGP showed amphibolite facies metamorphism at ~500-475-Ma. Based on geochronological data (Ravikant, 2019; Ganguly et al., 2021), it has been established that Cambrian-age metamorphism was induced by a W to NW thrusting event, which also reworked the older Grenvillian-age EGP crust. Nevertheless, the precise extent of this metamorphism within the EGP remains speculative, necessitating further in-depth research and detailed analysis. Nd model ages indicate that the boundary between the

Archean Bastar craton and the EGP is characterized by a wide shear zone (TBSZ) hosting a mixed rock types originating from both terranes. Within this suture zone, rocks of amphibolite facies from the Bastar craton appear to have experienced intense high-pressure granulite facies metamorphism, likely occurring around 500 Ma (Padmaja et al., 2021). It was further argued from petrological, geothermobarometric and P-T pseudosection studies in mafic granulites that the peak metamorphic conditions, occurring at 9.75 ± 0.5 kbar and 875 ± 30 °C, were attained through dehydration-melting processes involving amphibole in mafic protolith and biotite in quartzofeldspathic protolith along a clockwise P-T trajectory which is somewhat similar P-T condition reported from interior EGP except it has followed anticlockwise isobaric cooling from peak metamorphic temperature. This Cambrian-age structural event at the northwestern tip of the EGP is correlated with the effect of far-field stress generated by the Kuunga orogen (Boger, 2011) at the margin of Australia-Mawson-Crohn craton during final assembly of the supercontinent East Gondwana. The Cambrian age thermal event described in the present study from the monzosyenite vein that is ca. 490 Ma also testifies the same. However, in the present study no further detailed analysis have been carried out from these rocks.
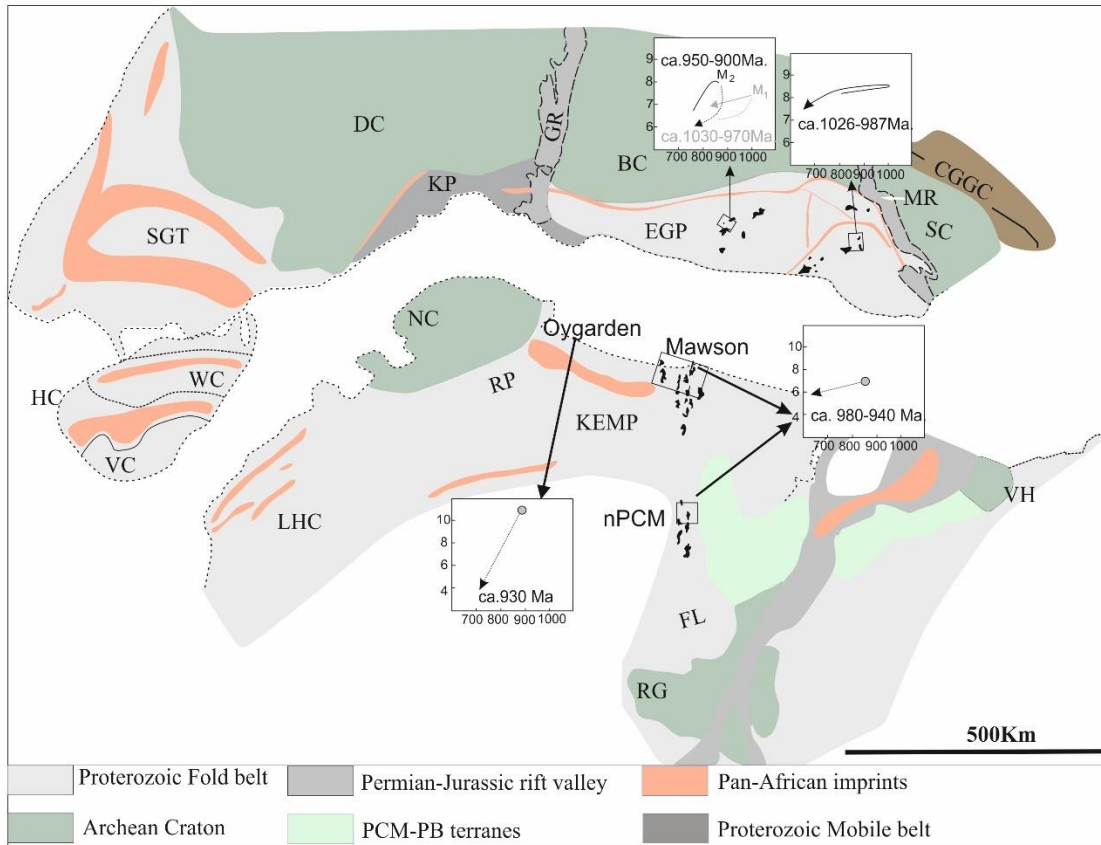
Fig. 8.1. Schematic diagram showing the reconstruction of the India-East Antarctica-Sri Lanka sector in the broad framework of the supercontinent East Gondwana (modified after Veevers, 2012). The representative P-T-t paths of the ca. 1000–900 Ma metamorphism from the EGP are from Bose et al. (2022) and Ganguly et al. (2018), while the same from the Rayner Province is from Harley (2003). Approximate locations of magmatic charn-ockite are shown in both the EGP (India) and the Rayner Province (East Antarctica). Abbreviations used: CGGC: Chotanagpur Gneissic Complex, SC: Singhbhum Craton, DC: Dharwar Craton, BC: Bastar Craton, MR: Mahanadi Rift, GR: Godavari Rift, SGT: Southern Granulite Terrain, WC: Wanni Complex, HC: Highland Complex, VC: Vijayan Complex, KP: Krishna Province, EGP: Eastern Ghats Province, LHC: Lutzow-Holm Complex, NC: Napier Complex, RP: Rayner Province, nPCM: Northern Prince Charles Mountains, FL: Fisher and Lambert terranes, RG: Ruker Group, VH: Vestfold Hills.
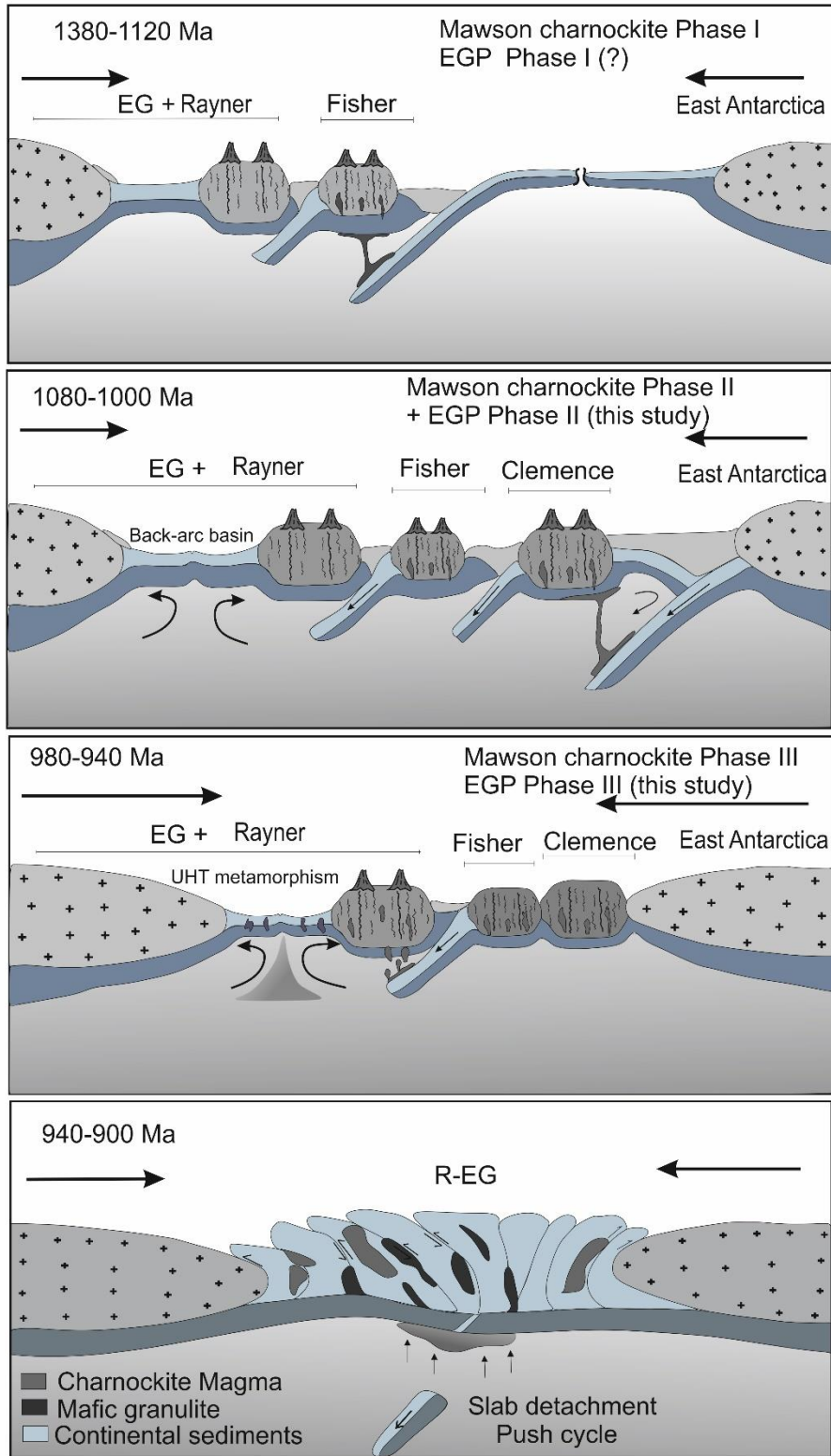
Fig.8.2. Cartoon diagram showing the tectonic development between India and East Antarctica during the time span of ca. 1380–900 Ma modified after Liu et al., (2014) and Bose et al. (2022). The cartoon shows phase-wise evolution of continental/magmatic arc in the sector and crystallization of charnockite magma in the Rayner-Eastern Ghats (R-EG) orogen. See text for details.